



This work is distributed under  
the Creative Commons Attribution 4.0 License.

Received: February 28, 2022

Revision received: June 6, 2022

Accepted: June 8, 2022

Published on line: October 12, 2022

Case study article

# Integration of geophysical information with geological cartography for mineral resources research and other applications in Colombia: examples from the Serranía de San Lucas, Antioquia Batholith and eastern Amazonia

Integración de información geofísica con cartografía geológica para investigación en recursos minerales y otras aplicaciones en Colombia: ejemplos en la serranía de San Lucas, Batolito Antioqueño y el oriente de Amazonía

Norma Marcela Lara<sup>1</sup>, Hernán Darío Arias<sup>1</sup>, Ismael Enrique Moyano<sup>1</sup>, Adriana Robayo<sup>1</sup>, Ernesto Gómez<sup>1</sup>, Diana Ospina<sup>1</sup>, Manuel Puentes<sup>1</sup>, Sergio Torrado<sup>1</sup>, Óscar Rojas<sup>1</sup>, Gloria Prieto<sup>1</sup>

1. Servicio Geológico Colombiano, Directorate of Mineral Resources, Bogotá, Colombia.

**Corresponding author:** Norma Marcela Lara Martínez, [nlara@sgc.gov.co](mailto:nlara@sgc.gov.co)

## ABSTRACT

Airborne geophysical information is used in the interpretation of geological features. The variations observed in airborne magnetic and gamma spectrometric data are used mainly to support the differentiation of geological units, to delimitate structures and to define compositional/lithological changes. In this context, the objective of this study is to support geological mapping through airborne magnetometry and gamma spectrometry geophysical data. Examples from two regions of the Colombian territory: a) the Serranía de San Lucas-Antioqueño Batholith and b) eastern Colombia are presented. Gamma spectrometric data are used to generate images of the K, U and Th channels in a ternary (RGB false color) map for the purpose of delimitate geological-geophysical domains. The magnetometry information was processed to highlight anomalous magnetic features and provide information about the structural framework of each of the areas of interest.

In the Serranía de San Lucas and Antioquia Batholith areas, 27 gamma spectrometric domains were interpreted primarily from the ternary composition images. Within these domains, a good correlation with each of the chronostratigraphic units was obser-

**Citation:** Lara, N. M., Arias, H. D., Moyano, I. E., Robayo, A., Gómez, E., Ospina, D., Puentes, M., Torrado, S., Rojas, O., & Prieto, G. (2021). Integration of geophysical information with geological cartography for research in mineral resources and other applications in Colombia: examples in the Serranía de San Lucas, Antioquia Batholith and eastern Amazonia. *Boletín Geológico*, 48 (Spl.1), 25-44. <https://doi.org/10.32685/0120-1425/bol.geol.48.Spl.1.2021.654>

ved, which enabled the identification and delimitation of areas with high or low concentrations of radioelements. In addition, the correlation of magnetic domains with high and low magnetic intensities and textures showed contrasts between igneous rocks, metamorphic rocks and sedimentary rocks. In the eastern zone, due to its fairly generalized geology, the geophysical information gained from both gamma spectrometry and magnetometry serves as a support to refine and delimitate the present geological units as well as their structural framework.

**Keywords:** airborne geophysics, gamma spectrometric data, magnetic data, chronostratigraphic units, ternary composition.

## RESUMEN

La información geofísica aerotransportada es una herramienta para la interpretación de características geológicas. Las variaciones que se observan en los datos magnéticos y gamma espectrométricos aerotransportados son utilizados, principalmente, como apoyo para diferenciar unidades geológicas, delimitar estructuras y limitar cambios composicionales. En este contexto, el objetivo de este estudio es dar soporte al mapeo geológico a partir de los datos de geofísica aerotransportada de magnetometría y gamma espectrometría en dos regiones del territorio colombiano: a) serranía de San Lucas-Batolito Antioqueño, y b) oriente colombiano. El procesamiento de los datos gamma espectrométricos consiste en generar imágenes de los canales de K, U y Th, además de una composición ternaria en falso color RGB de estos tres canales, con la finalidad de delimitar dominios geológicos-geofísicos. De otro lado, la información de magnetometría se procesa para resaltar características magnéticas anómalas y proveer información acerca del marco estructural de cada una de las áreas de interés.

En la zona comprendida en la serranía de San Lucas-Batolito Antioqueño se delimitaron 27 dominios gamma espectrométricos, interpretados especialmente a partir de las imágenes de composición ternaria; en ellos se observa una buena correlación con la composición de cada una de las unidades litoestratigráficas, lo que permite identificar y delimitar zonas con altas o bajas concentraciones de radioelementos. Además, la correlación de dominios magnéticos con altas y bajas intensidades y texturas magnéticas muestra contrastes entre rocas ígneas, rocas metamórficas y rocas sedimentarias. Por su parte, en la zona oriental, por tener una geología bastante generalizada, la información geofísica, tanto de gamma espectrometría como de magnetometría, sirve de apoyo para depurar y delimitar con mayor exactitud temática las unidades geológicas presentes, así como su marco estructural.

**Palabras clave:** geofísica aerotransportada, datos gamma espectrométricos, datos magnéticos, unidades cronoestratigráficas, composición ternaria.

## 1. INTRODUCTION

Currently, high-resolution airborne geophysical data are available and also it is possible to process and interpret large amounts of data, which has increased the volume of geological information supported by geophysical information (Isles and Rankin, 2013). This results in maps and products that allow to establish the continuity and to defining with greater precision the boundaries between geological units when considering the interpretation of geophysical features.

Different types of data are used to produce geological maps. Some data are obtained during geological data collection campaigns in the field, while others consist of geochemical data, aerial photographs and satellite images. The integration of geological and geophysical data helps to improve the visualization of geological and structural features, from which structures

and lineaments are identified, in addition to serving as support data for the delimitation of rocks.

Since 2012, the Servicio Geológico Colombiano (SGC) has advanced airborne surveys for the collection of geophysical data in areas of interest in the Colombian territory through magnetometry and gamma spectrometry; as a result, large regional coverage with high spatial resolution data was achieved (Moyano et al., 2020). Until 2020, the information obtained in these surveys was compiled in seventeen blocks that cover approximately 520 000 square kilometers of Colombian territory, distributed in the Caribbean, Andean, Amazonian and Orinoquia areas (Figure 1).

For the present work, two study areas were selected for the integration of geophysical information with the available geological cartography, these areas are: the Serranía de San Lucas-Antioquia Batholith and the eastern Colombian zone.



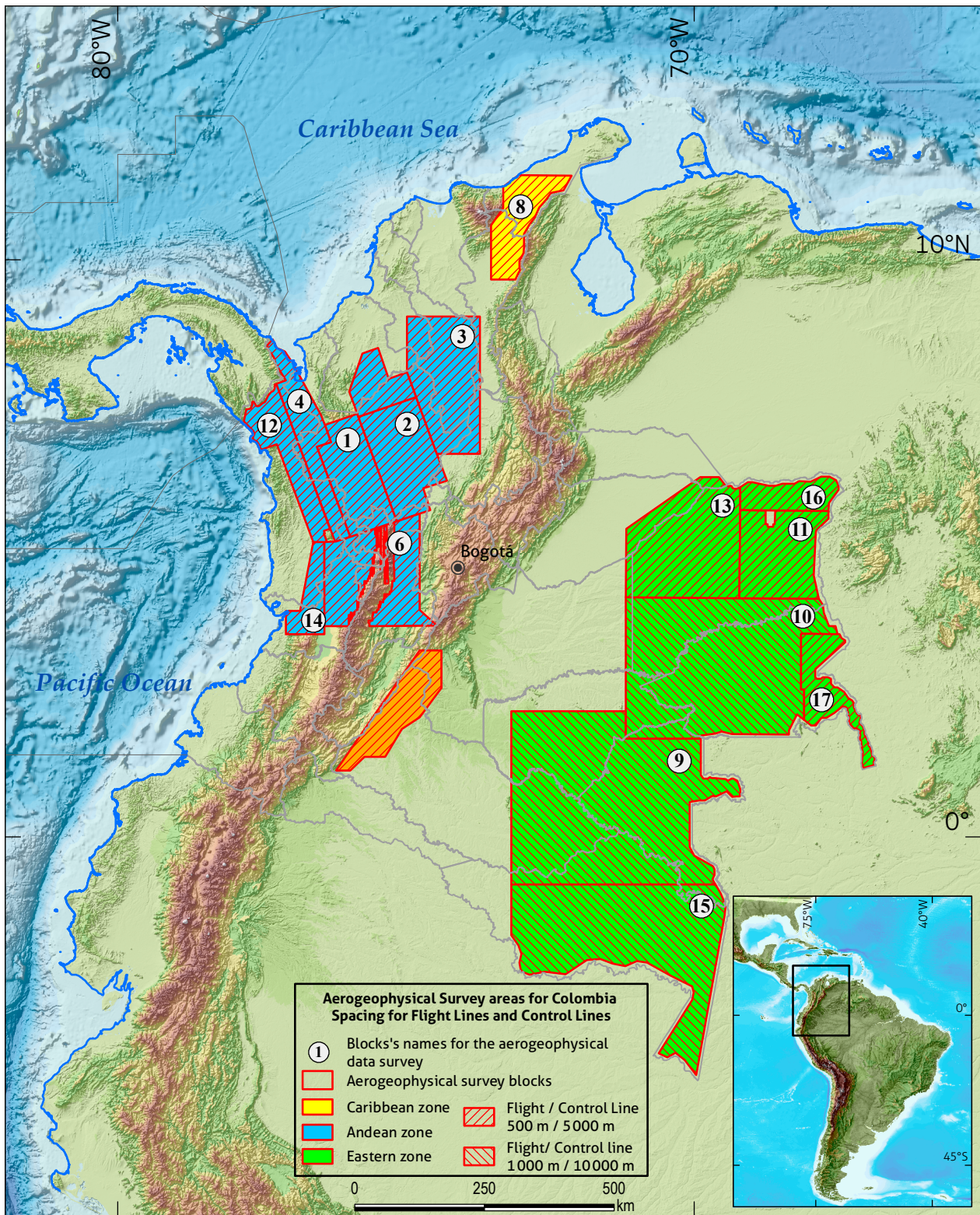


**Figure 1.** Ariborne geophysical blocks of Colombia, 2020

1. Antioquia\_W, 2. Antioquia\_E, 3. Bolívar, 4. Urabá, 6. Andes\_N, 8. Cesar-Perijá, 9. Amazonas\_N, 10. Guanía, 11. Vichada, 12. Darién, 13. Vichada\_W, 14. Buenaventura, 15. Amazonas\_S, 16. Vichada\_N, 17. Guainía\_E, 18. Garzón, 19. Córdoba.



The magnetometry data were processed qualitatively and semiquantitatively by the application of supervised classification methodologies for the delimitation and characterization of geophysical features domains. Magnetic structures were characterized through techniques for the automatic detection of lineaments, and gamma spectrometric domains were generated with radiometric information and multivariate spatial analysis. The layers of information obtained were integrated with the available regional geological cartographic data (Gómez et al., 2015) for the purpose of obtaining information to identify areas with the potential existence of mineral resources and other applications, such as the validation and complementation of geological cartography.

## 2. GEOLOGICAL FRAMEWORK

### 2.1. Area 1. Serranía de San Lucas-Antioquia Batholith

The area of the Serranía de San Lucas-Antioquia Batholith is located in the northwest of Colombia, in the departments of Antioquia, Bolívar, Boyacá, Caldas, Cesar, Córdoba, Magdalena and Sucre. The region is in the confluence zone of the Cen-

tral and Western mountain ranges, and has heights that vary between 0 m.a.s.l. and 3700 m.a.s.l. The area is dominated by two topographically abrupt regions: in the central northern part, by the Serranía de San Lucas mountain range, and toward the southwestern part, in the Antioquia area, by the Central Cordillera. The study area is framed by the Cauca River to the west and Magdalena River to the east (Figure 2).

### 2.2. Area 2. Eastern Colombia

The area of eastern Colombia is located in the eastern part of the country and includes the departments of Amazonas, Arauca, Caquetá, Casanare, Guainía, Guaviare, Meta, Vaupés and Vichada. The area includes the Guiana Shield, with heights varying between 0 m.a.s.l. and 900 m.a.s.l. The area is characterized by a flat topography, to the north dominated by the savannas of the Llanos Orientales; in the central area present the hills of Mapi-ripiana, El Tigre and Caño Minas, and the Serranía de Naquén; and for the Amazon area, the mountains of Chiribiquete, Aracuaara and La Trampa. The study area is framed by large bodies of water, such as the Meta, Orinoco, Guaviare, Vichada, Inírida, Vaupés, Apaporis, Caquetá and Putumayo rivers (Figure 3).

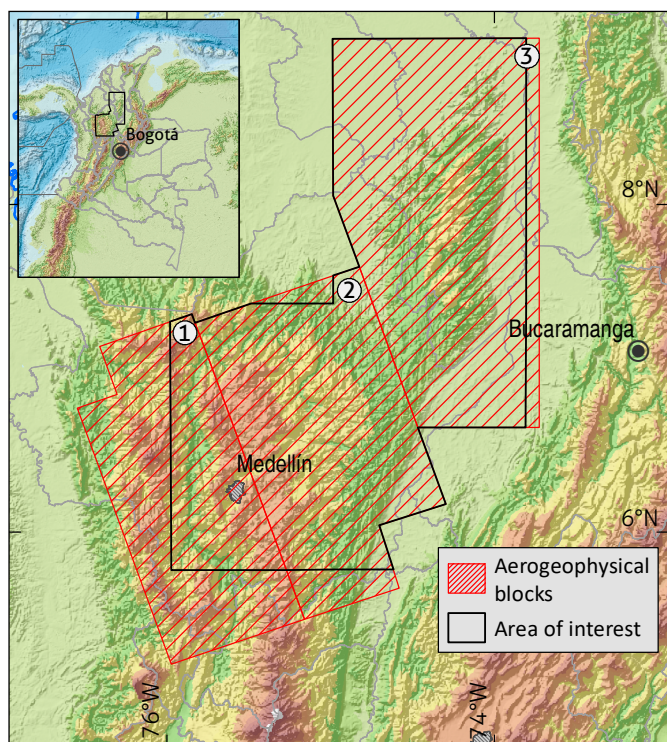


Figure 2. Geographic location of area 1: the Serranía de San Lucas-Antioquia Batholith

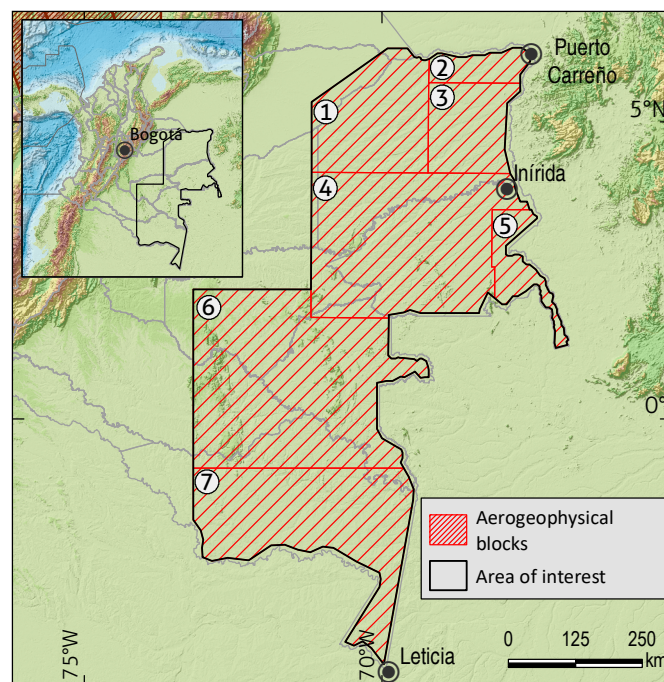


Figure 3. Geographic location of area 2: eastern Colombia

**Table 1.** Parameters for the acquisition of airborne geophysical information for each of the areas of interest

	Aerogeophysical block	Sampling interval	Flight lines/dir. flight lines	Control lines/dir. control lines	Flight altitude	Acquisition date	Area (km <sup>2</sup> )
Serranía de San Lucas-Antioquia Batholith	Antioquia_W	80 m (gamma)	500 m/N20W	5000 m/N70E	100 m	18-10-2014	7967
	Antioquia_E					15-08-2014	20710
	Bolivar	8 m (mag)	500 m/NS	5000 m/EW		14-12-2013	29716
Eastern Colombia	Amazonas_N	80 m (gamma)	1000 m/NS	10 000 m/EW	100 m	25-07-2014	114393
	Amazonas_S					23-06-2015	72510
	Guainia	8 m (mag)	500 m/NS	5000 m/EW		15-11-2014	92616
	Guainia_E					16-09-2016	12414
	Vichada	8 m (mag)	500 m/NS	5000 m/EW		24-06-2014	25080
	Vichada_N					12-03-2016	9724
	Vichada_W					17-06-2016	42881

### 3. MATERIALS AND METHODS

#### 3.1. Airborne geophysical information

Since 2012, the SGC acquired airborne geophysical data by magnetometry and gamma spectrometry geophysical methods in areas of interest in the Colombian territory. This information has been collected using an airborne platform (airplanes) at a height of 100 meters above the ground, as allowed by the topography and safety precautions. Table 1 presents general information on the blocks covered. Additional details about this information and characteristics of the data are found in Moyano et al. (2020).

#### 3.2. Data processing

Initially, the spatial distribution of the data was reviewed to verify the continuity and coupling between the different blocks. Subsequently, the gamma spectrometry data were refined to exclude the areas where a greater flight height affected the quality of the information by exceeding the sensitivity limit of the instruments.

The final images were processed by 2D interpolation in regular grids through minimum curvature for the gamma data and bidirectional gridding for the magnetometry data (Moyano et al., 2020). The cell size used followed the recommendations of Gunn et al. (1997) with respect to using cell values between one quarter ( $\frac{1}{4}$ ) and one eighth ( $\frac{1}{8}$ ) of the nominal spacing of the flight lines; this aims to avoid loss of information and, therefore, to recover all frequencies.

According to the specifications of the blocks in each work area (Table 1), the cell size was defined as a quarter ( $\frac{1}{4}$ ) of the distance between the flight lines, as follows:

1. *Serranía de San Lucas-Antioquia Batholith*. The cell size for the interpolation of the images was selected at 125 m, since

all the aerogeophysical blocks involved in the area have a flight line spacing of 500 m.

2. *Eastern Colombia*. The cell size used for the interpolation of the data was 250 m. In this area, there are three aerogeophysical blocks for which information was acquired in lines with spacing of 1000 m. Although information on the four blocks in this area was acquired with a spacing of 500 m, the information was generalized so as not to force an interpolation that would result in artifacts in the interpolated data.

##### 3.2.1. Gamma spectrometry data

The airborne gamma spectrometric method is based on the detection of the natural gamma radiation emitted due to the process of stabilization of the nuclei in the radioactive elements in the materials and rocks on the Earth's surface. Among these elements, potassium (K), uranium (U) and thorium (Th) are the only natural elements with radioisotopes that produce gamma rays of sufficient energy and intensity to be measured in airborne geophysics surveys (International Atomic Energy Agency, 2003). Given that gamma rays are strongly attenuated in rocks, soil and air, most of the radiation emanates from shallow soil (approximately 90% of the measured gamma rays are received from 30 cm to 50 cm below the surface).

Because the three radioelements measured have specific chemical affinities, their distributions in rocks vary as a function of parameters such as mineralogy, oxidizing conditions, hydrothermalism and weathering. For this reason, K, U and Th can have very variable concentrations in rocks, which can be used to support geological cartography (Martelet et al., 2006).

The gamma spectrometry layers generated correspond to maps of equivalent concentrations of K, U and Th (Figures 4 and 5). From these three maps, a ternary composition was made in false RGB color (R: *red*, associated with channel K; G: *green*,



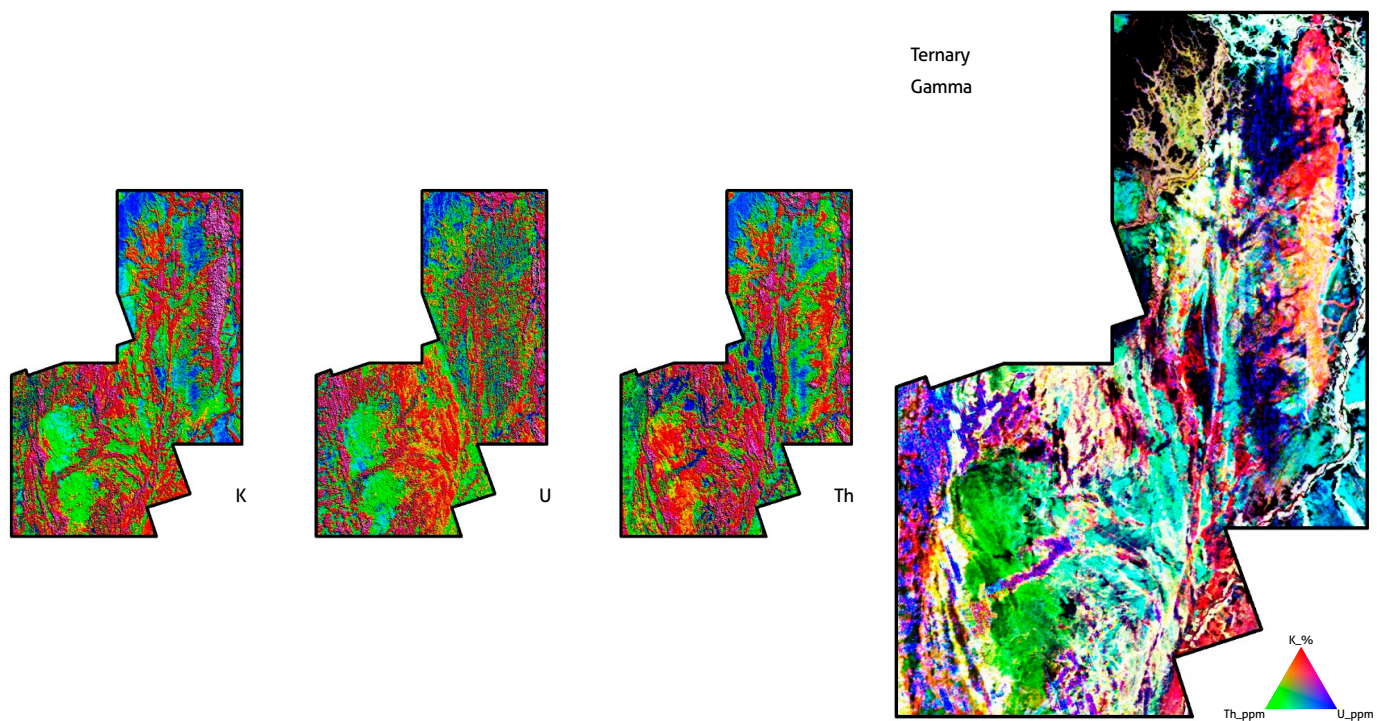


**Figure 4.** Flowchart of the gamma spectrometric data of area 1: Serranía de San Lucas-Antioquia Batholith  
 K: Potassium; U: uranium; Th: thorium; ternary gamma: RGB false color ternary composition of the K, U and Th channels.

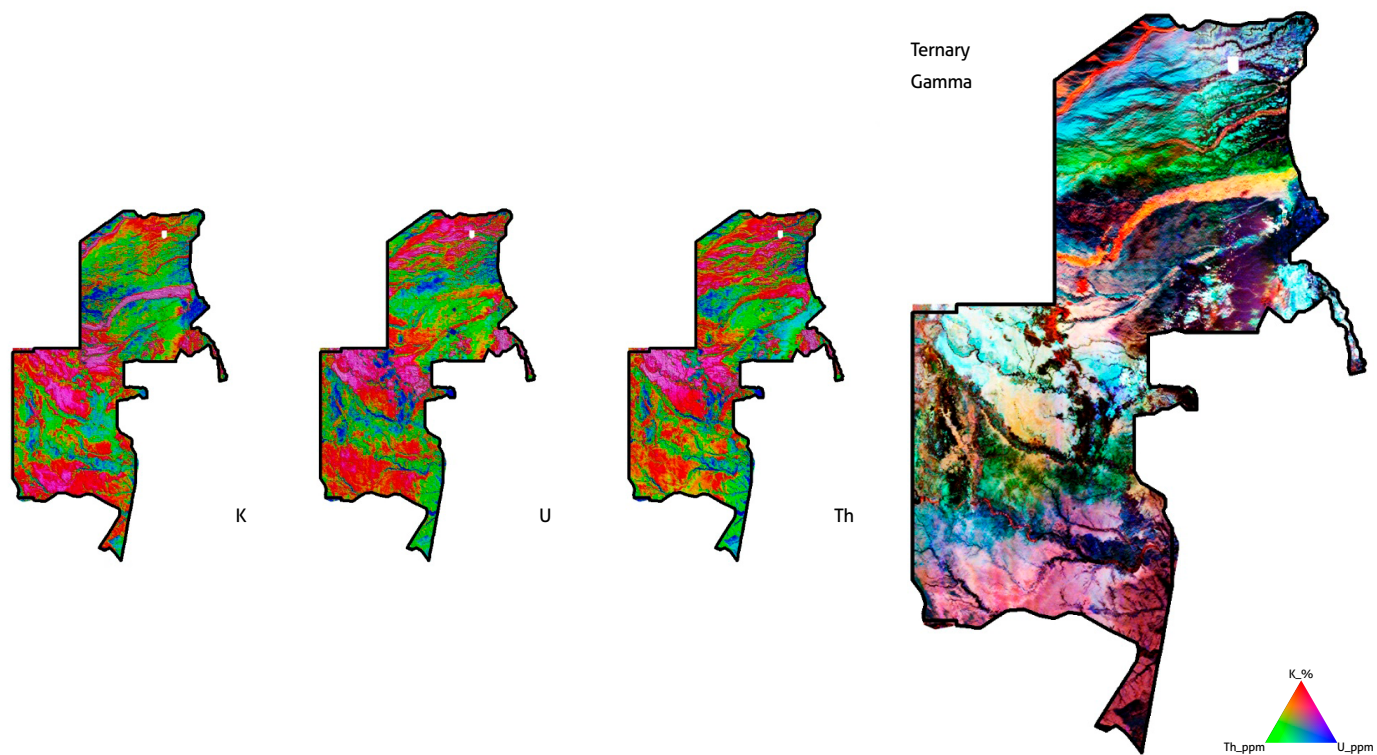


**Figure 5.** Flowchart of the gamma spectrometric data obtained in area 2: eastern Colombia  
 K: Potassium; U: uranium; Th: thorium; ternary gamma: ternary composition in false color RGB of the K, U and Th channels.

associated with channel Th; B: *blue*, associated with channel U). This ternary composition map is very useful, since the combination of the colors represents the average concentration of the three elements: white colors show areas that are high in the three radioelements, while dark brown or black colors indicate areas that have low contents. Low radiometric values are generally associated with rocks with low contents of radioactive elements or the presence of water masses or saturated soil. In addition, the radiometric images were integrated with a digital terrain model (DTM), generated from the altimetry data obtained during the survey of geophysical information, to observe the effect of the topography on the distribution of the radioelements.

### 3.2.2. Magnetometry

The total field magnetic anomaly (TMA) represents the portion of the observed magnetic field that does not correspond to the Earth's magnetic field reference model (International Geomagnetic Reference Field [IGRF]) (Thébault et al., 2015) nor to external temporal effects such as solar storms and diurnal variation. Therefore, the TMA can be associated with the effects of the geomagnetic field due to variations in the distribution of magnetization in the Earth's crust caused by changes in the concentration of magnetic minerals in the rocks that comprise it.

Due to the dipolar nature of the magnetic field, the TMA represents magnetic anomalies (areas where the concentration of magnetic minerals is higher or lower than that in the environment) as dipoles. To establish a monopolar analog, transformations such as reduction to the magnetic pole (RTP) transform the dipole anomaly into a single peak on the body that is causing it, as if it were located in a magnetic pole. The RTP then transforms the asymmetric anomalies into symmetrical anomalies and locates them on the causative bodies (Marangoni, 2014). Other transformations used are the analytical signal (AS), which highlights the lateral contrasts (contours) of the anomalous source; the tilt derivative (Tilt), which highlights linear features of the information; and vertical derivatives (Dz), which, according to their magnitude, enhance progressively shallower attributes in the information. All these data processing steps are proposed to enhance features of the original information, such as structures and lateral changes, in support of the structural interpretation of the area.

An additional processing step used is the creation of a ternary composition (RGB) image from images of vertical derivatives in three different orders. That composite image allow

to discriminate different *magnetic domains* (MD) from the delineation of areas of high magnetization (or high frequencies) and areas of low magnetization (or low frequencies), as well as lateral contrasts in the texture (e.g., high content of high frequency or *rough* anomalies). For the area of the Serranía de San Lucas-Antioquia Batholith, the orders generated correspond to 0.5 Dz-0.75 Dz-1 Dz (Figure 6), and for the eastern Colombian zone, they correspond to 0.75 Dz-1 Dz-1.25 Dz (Figure 7). The difference in the orders of the derivatives for the two areas is due to the greater amount of high frequencies associated with the topography of the Andean zone.

For the characterization of the structural framework of the areas of interest (magnetic lineaments), the images of the tilt derivative (Tilt) and the analytical signal were used. The first highlights the lineaments and detects the edges of the geological features that may be associated with fractures, faults, or geological contacts. In addition, it is very useful to delimit both shallow and deep sources (Miller y Singh, 1994). The analytical signal better defines the limits of the magnetic source, which contributes to the geometrical and spatial characterization of the various magnetic sources, according to the intensity of the magnetic field.

## 4. RESULTS

### 4.1. Gamma spectrometric domains

Geological mapping techniques have progressively evolved toward the combination of field observations and remote sensing approaches. The use of techniques such as gamma ray spectrometry allows the identification of radioelement concentration patterns in combination with geological observations in the field. In addition, the continuous coverage of these geophysical data is crucial to extrapolate point observations of the soil to an entire region.

As the use of geographic information systems (GIS) software has become widespread, allowing better analysis of spatial relationships between datasets (geological, geophysical, geochemical, etc.), which has made it possible for geological mapping to present greater thematic precision. However, with the increase in the number of available data layers, this qualitative approach has become difficult to apply and requires the implementation of automated procedures, such as multivariate analysis, which was developed for aiding interpretation in cases in which the number of available variables increases progressively as more information is collected.

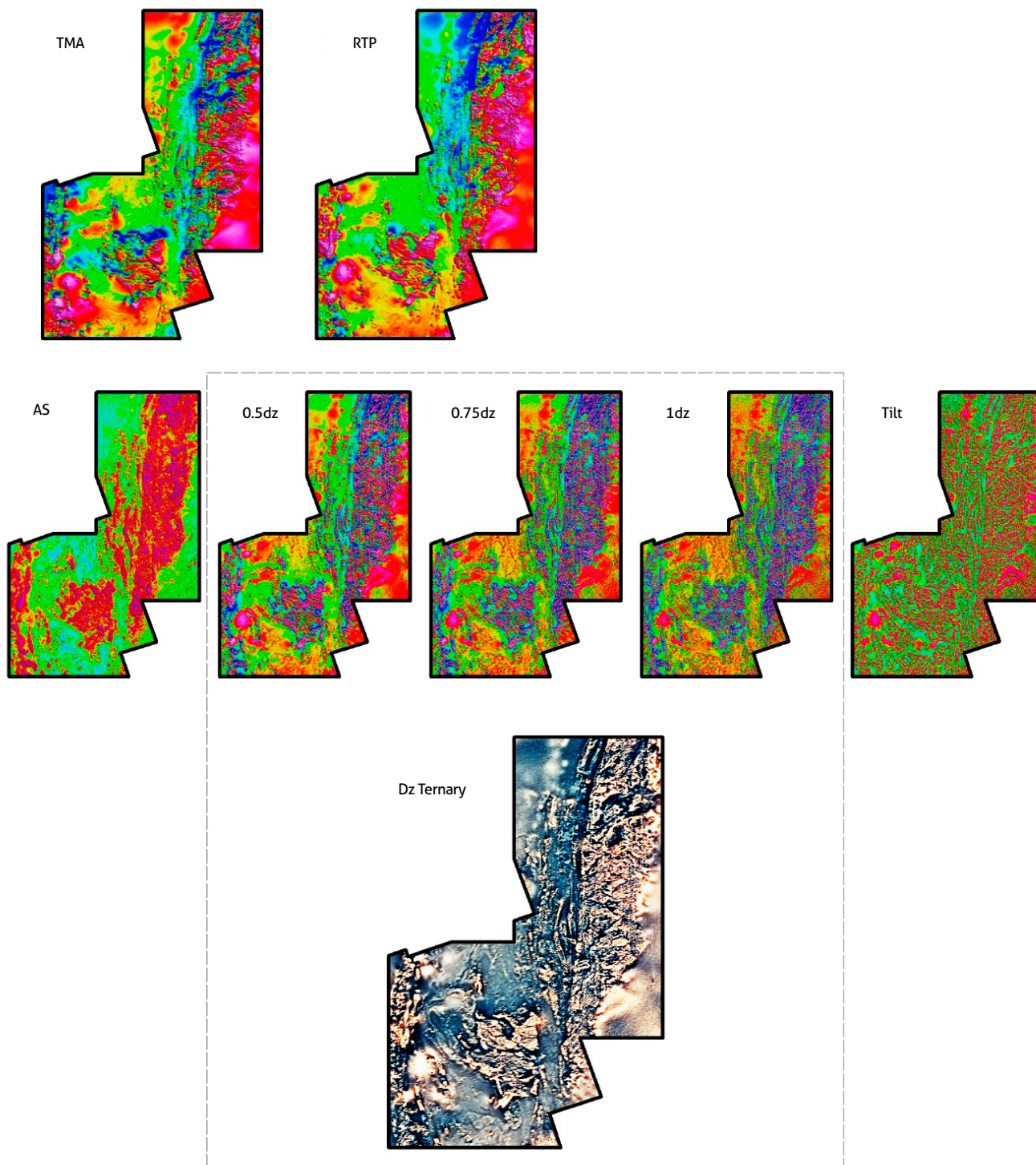


**Figure 6.** Flow diagram of the magnetic data of area 1: Serranía de San Lucas-Antioquia Batholith  
TMA: total field magnetic anomaly; RTP: reduction to the pole of the total field magnetic anomaly; AS: analytical signal of the RTP; Dz: Ternary image from the 0.5, 0.75 and 1 vertical derivatives from the RTP; TILT: Tilt derivative; ternary Dz: ternary RGB composition of the vertical derivatives 0.5-0.75-1.



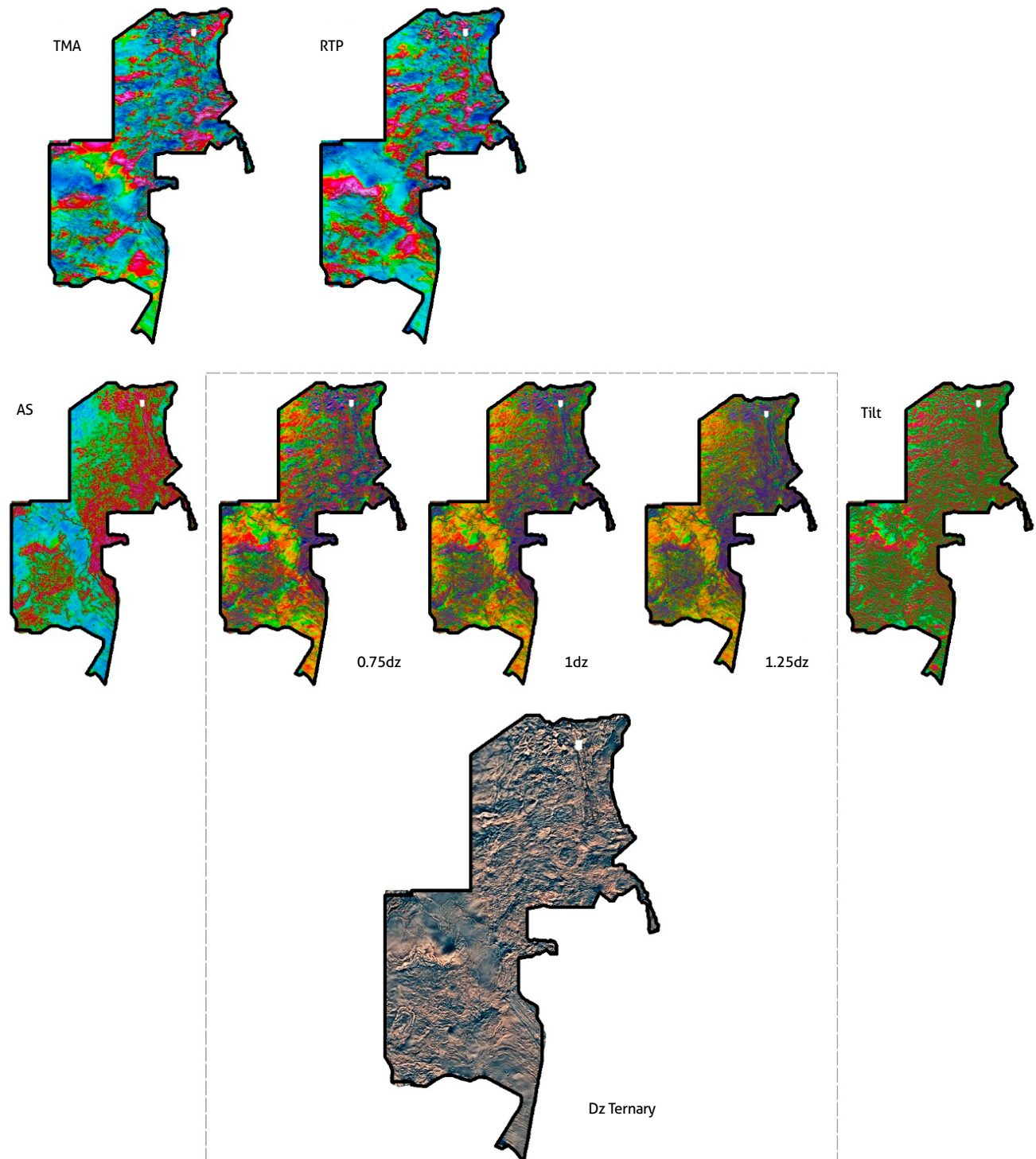


**Figure 7.** Flowchart of the magnetic data of area 2: eastern Colombia  
TMA: total field magnetic anomaly; RTP: reduction to the pole of the total field magnetic anomaly; AS: analytical signal of the RTP; Dz: vertical derivatives from the RTP; TILT: Tilt derivative; ternary Dz: ternary RGB composition of the vertical derivatives 0.75-1-1.25.



#### 4.1.1. Multivariate spatial analysis: classification methods

Among the widely known *classification algorithms*, two approaches are established: supervised and unsupervised classifications. In unsupervised classification, or *clustering*, image processing software automatically computes the values of different coverages and groups them according to their spectral values. In supervised classification, the spectral values of different covers are computed through training zones, which generally correspond to sites previously sampled in the field or for which there is previous knowledge (Richards, 2013)

Supervised classification requires a set of classes defined by an analyst, in addition to the characteristic spectral signatures of the classes. The approach developed for the two areas of interest relied on a supervised classification approach that is based on statistics, in which each class was assigned the highest probability in the dataset (supervised classification of maximum likelihood). Patterns of high, medium and low contents of each of the radioelements (K, U, Th) were previously identified in the interpolated images, and these patterns were used as training zones (Killeen et al., 2015).

#### 4.1.2. Supervised maximum likelihood classification method

The supervised maximum likelihood classification method is one of the most frequently used classification methods. In this approach, a pixel is assigned to the class with the highest probability, according to its spectral characteristics previously defined by the analyst. The maximum likelihood algorithm is trained by control points, which it considers parameters. Subsequently, the algorithm selects the values of a finite set of data (in this case, the processed and interpolated gamma spectrometry images) with a greater probability of approaching the parameter defined in advance and then groups these data into clusters, with the same values reclassified into topics or classes; that is, the parameters that maximize the likelihood function are clustered.

The classification of maximum likelihood is also known as *classification by the Bayesian algorithm*, since *a priori* probabilities can be assigned by means of Bayes's theorem, which expresses the probability of a random event *A* occurring in *B* (Japan Association on Remote Sensing, 1993), according to (1):

$$P(A_i|B) = \frac{P(B|A_i)P(A_i)}{\sum_{i=1}^n P(B|A_i)P(A_i)} \quad (1)$$

The maximum likelihood method has an advantage from the point of view of probability theory, but care must be taken with the following issues (Japan Association on Remote Sensing, 1993):

1. The samples used as training sites should be sufficient to allow the estimation of the mean vector and the variance-covariance matrix of the population.
2. The inverse matrix of the variance-covariance matrix becomes unstable when there is a very high correlation between two bands or the terrain data are very homogeneous. In these cases, the number of bands must be reduced by principal component analysis.

#### 4.1.3. Application of the supervised maximum likelihood classification method

In the images created by minimum curvature interpolation (Yang et al., 2004) for each of the elements (K, U and Th), three main classes were defined: high concentrations, medium concentrations, and low concentrations. Once defined, the training zones were established in each image, with sufficiently high and homogeneous sampling in each image so that the spectral signatures were well defined. Subsequently, the maximum likelihood algorithm was applied, and it was verified that there was low correlation in the variance-covariance matrices. In this way, the maximum statistical probability was established for each cell of the images (K, U and Th), and the class to which the cells belonged was defined.

The steps involved in the processing and analysis of the data to generate the spectrometric gamma domains (GDs) are detailed in Figure 8. The processing software was ArcGIS 10.6 (the "Spatial Analysis" tool was used).

Once each image was classified, the gamma spectrometric domains of the areas of interest were defined. Given that there are three elements (K, U and Th) and that each element was assigned to three classes (high, medium, and low), it was possible to establish up to twenty-seven possible combinations in the area of interest (Figures 9 and 10; Table 2).

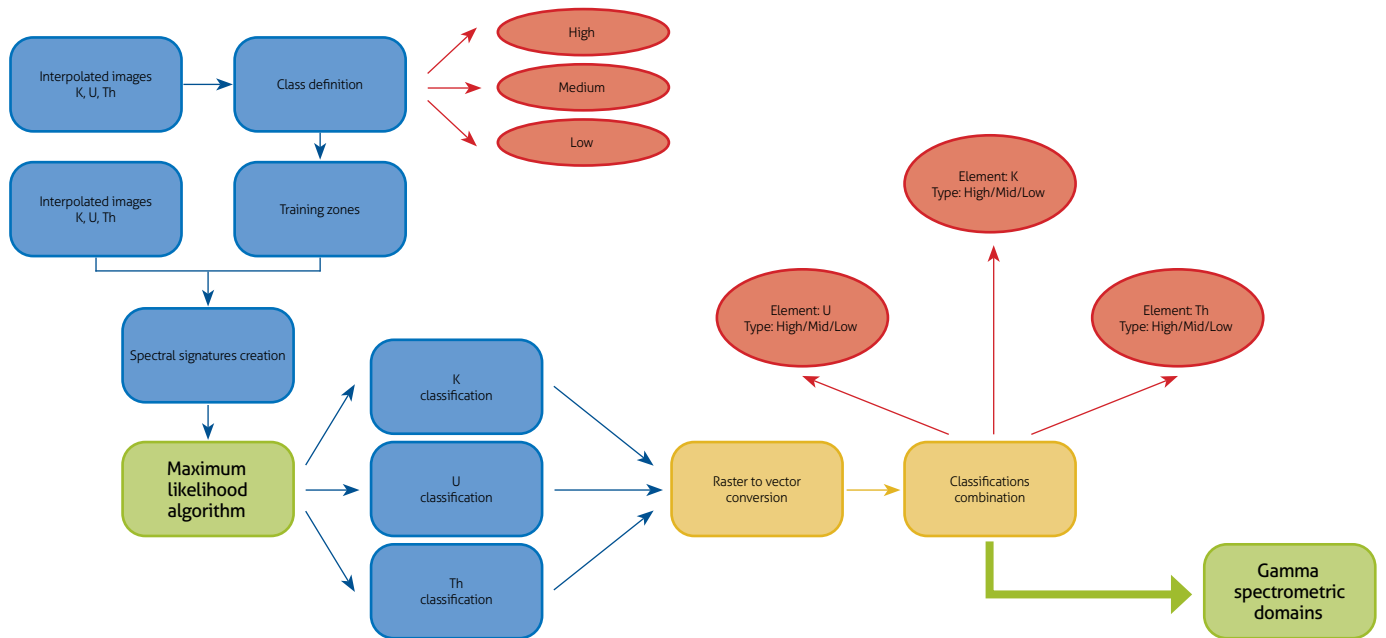


Figure 8. Flowchart of the application of the supervised classification method to obtain gamma spectrometric domains in the areas of interest: Serranía de San Lucas-Antioqueño Batholith and eastern Colombia

Table 2. Description of the gamma spectrometric domains generated for the areas of interest: Serranía de San Lucas-Antioquia Batholith and eastern Colombia

Domain	Combination	Detail			Code	Color
		Potassium (K)	Uranium (U)	Thorium (Th)		
1	Kh-Uh-Thh	High	High	High	333	
2	Kh-Uh-Thm	High	High	Medium	332	
3	Kh-Uh-Thl	High	High	Low	331	
4	Kh-Um-Thh	High	Medium	High	323	
5	Kh-Um-Thm	High	Medium	Medium	322	
6	Kh-Um-Thl	High	Medium	Low	321	
7	Kh-UL-Thh	High	Low	High	313	
8	Kh-UL-Thm	High	Low	Medium	312	
9	Kh-UL-Thl	High	Low	Low	311	
10	Km-Uh-Thh	Medium	High	High	233	
11	Km-Uh-Thm	Medium	High	Medium	232	
12	Km-Uh-Thl	Medium	High	Low	231	
13	Km-Um-Thh	Medium	Medium	High	223	
14	Km-Um-Thm	Medium	Medium	Medium	222	
15	Km-Um-Thl	Medium	Medium	Low	221	
16	Km-UL-Thh	Medium	Low	High	213	
17	Km-UL-Thm	Medium	Low	Medium	212	
18	Km-UL-Thl	Medium	Low	Low	211	
19	Kl-Uh-Thh	Low	High	High	133	
20	Kl-Uh-Thm	Low	High	Medium	132	
21	Kl-Uh-Thl	Low	High	Low	131	
22	Kl-Um-Thh	Low	Medium	High	123	
23	Kl-Um-Thm	Low	Medium	Medium	122	
24	Kl-Um-Thl	Low	Medium	Low	121	
25	Kl-UL-Thh	Low	Low	High	113	
26	Kl-UL-Thm	Low	Low	Medium	112	
27	Kl-UL-Thl	Low	Low	Low	111	

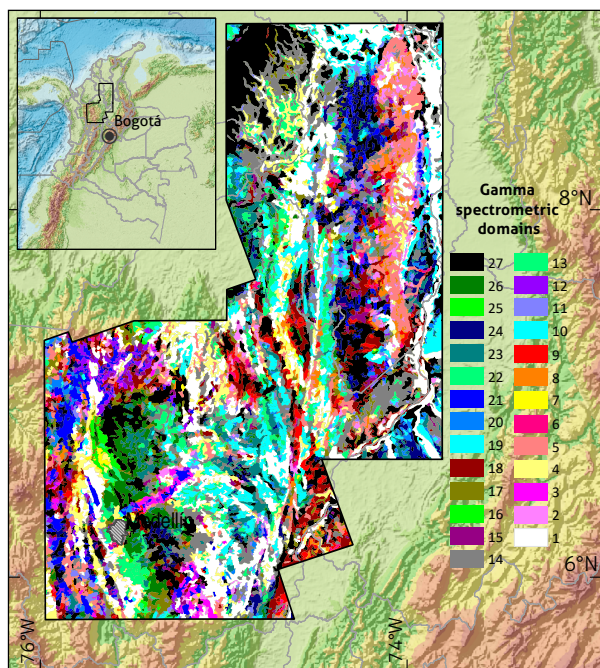


Figure 9. Gamma spectrometric domains in the Serranía de San Lucas-Antioquia Batholith area

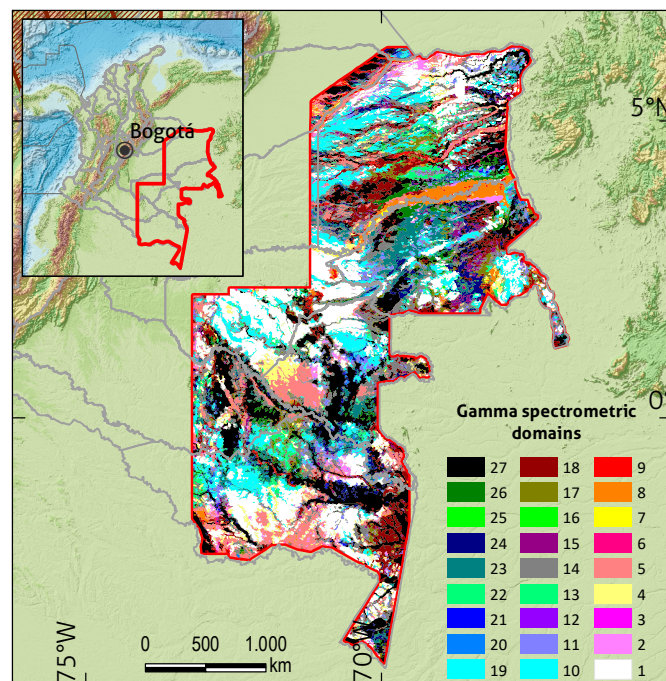


Figure 10. Gamma spectrometric domains in eastern Colombia

#### 4.2. Magnetic domains (MDs)

Magnetic domains are areas with similar magnetic features, delimited by taking into account two magnetic characteristics: texture and intensity. Magnetic domains are delineated from the vertical gradient of the magnetic field, called the *vertical derivative* ( $D_v$ ). This transformation enhances shallow magnetic sources while attenuating or suppressing the deep sources as the order of the derivative increases (Reeves, 2005).

The magnetic characteristics that allow the delimitation of the magnetic domains (MD) are: a) the magnetic intensity, related to the amplitude of the signal, and defined in three clas-

ses: high, medium, and low intensity; b) the magnetic texture, with which the *roughness* of the magnetic clusters in each image is discriminated. The magnetic texture is related to the power spectrum of the magnetic signal: high frequencies produce rough textures, and low frequencies produce smooth textures.

Once the domains were obtained by grouping the intensity and magnetic texture, the information was combined by means of cartographic generalization procedures and delimitation of domain borders. The combination of the two attributes resulted in the delimitation of nine MDs (Figures 11 and 12), the details of which are shown in Table 3.

Table 3. Description of the magnetic domains generated for the areas of interest: Serranía de San Lucas-Antioqueño Batholith and eastern Colombia

Domain	Detail				Code	Color
	Intensity		Texture			
	Class	Code	Type	Code		
1	High	3	Rough	3	33	
2	High	3	Medium	2	32	
3	High	3	Soft	1	31	
4	Medium	2	Rough	3	23	
5	Medium	2	Medium	2	22	
6	Medium	2	Soft	1	21	
7	Low	1	Rough	3	13	
8	Low	1	Medium	2	12	
9	Low	1	Soft	1	11	



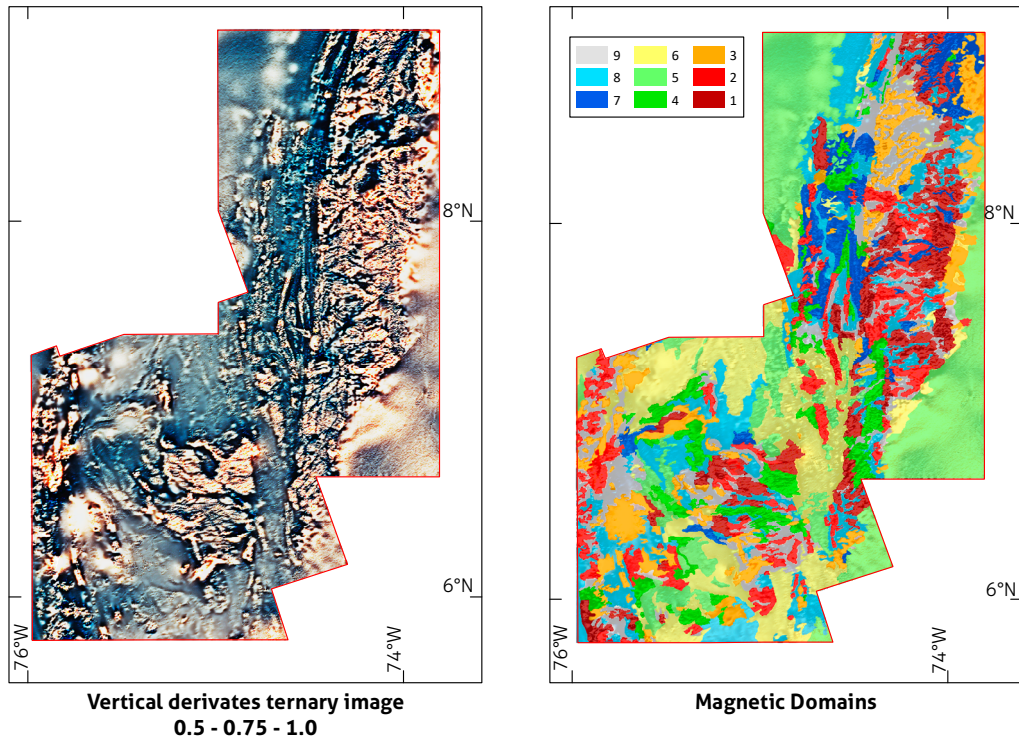


Figure 11. Magnetic domains of the Serranía de San Lucas-Antioquia Batholith area

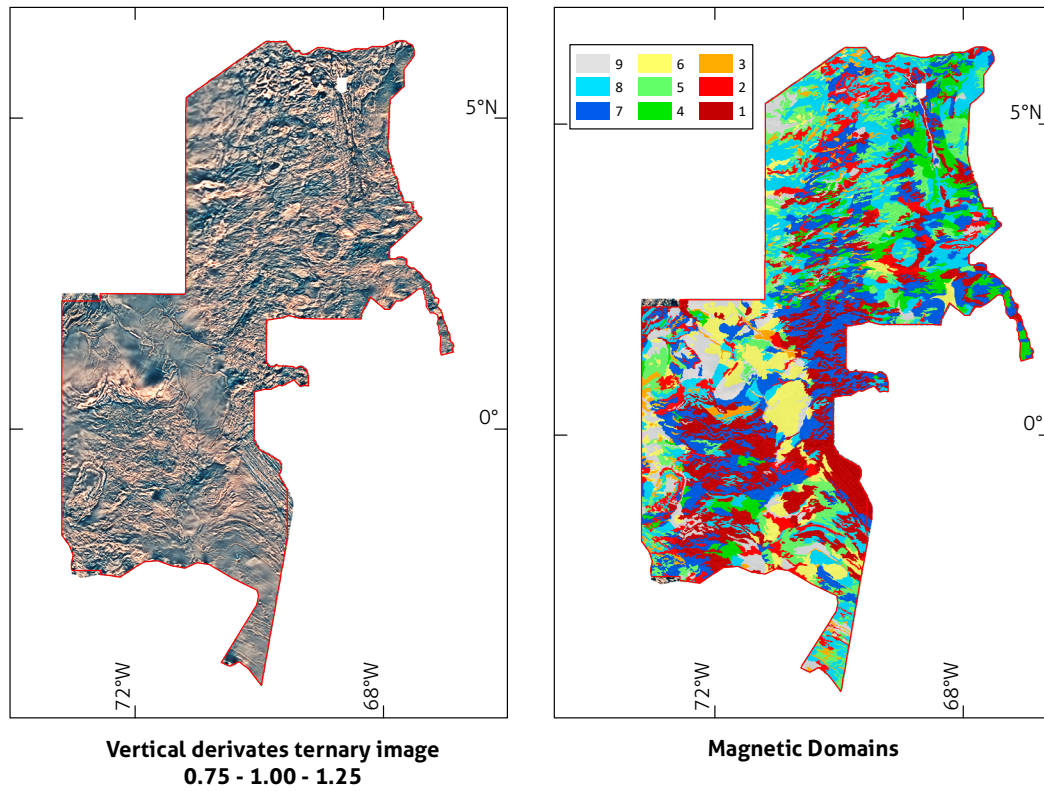


Figure 12. Magnetic domains of eastern Colombia

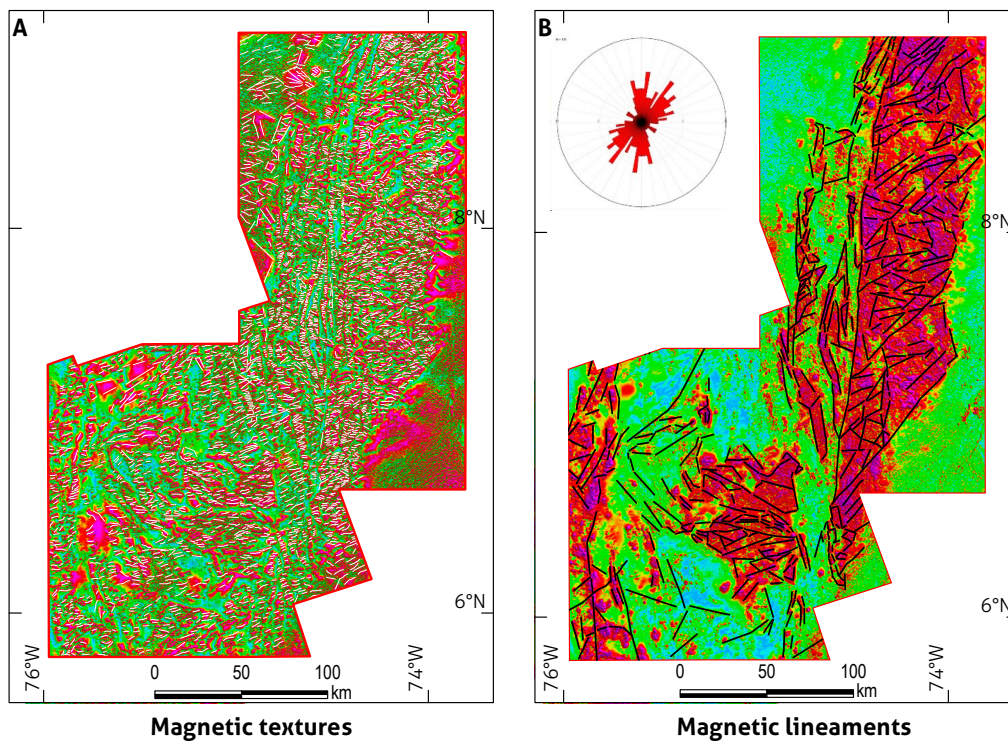


Figure 13. a) Magnetic lineaments on the analytical signal image and b) Rose diagram corresponding to the area of the Serranía de San Lucas-Antioquia Batholith

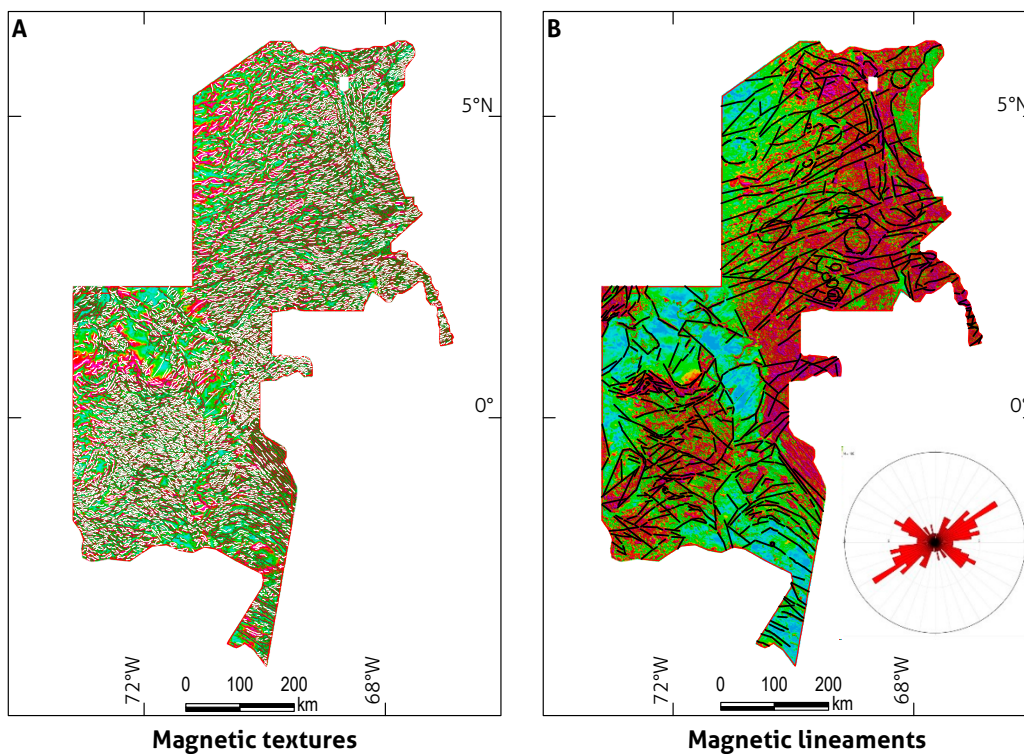


Figure 14. a) Magnetic lineaments on the analytical signal image; b) Rose diagram corresponding to eastern Colombia



### 4.3. Magnetic lineaments

From aeromagnetic data, magnetic lineaments that delineate the lateral changes in the magnetic field and represent the structural trends of each zone were selected. The lineaments are attributable to changes in the magnetic susceptibility of the rocks, possibly limited by structural and lithological controls, such as faults and fractures, among others.

The determination of the magnetic lineaments was performed through a quantitative and semiautomated process with the use of the CET (Center for Exploration Targeting) Grid Analysis tool (Abbass y Mallam, 2013). This allowed the automatic detection of lineaments through texture analysis while suppressing low values and preserving the orientation and local maximum amplitude values. In addition, it delimited the edges of the magnetic anomalies. The phase analysis detects regions with continuous linear trends and estimates of trend lines from the information detected by the phase analysis can reveal lithological and structural contrasts, mainly from the

image created by the Tilt derivative. The result is a set of vectorized linear segments that show changes in orientation and regional structures within the area.

Once the magnetic lineaments were obtained from the CET, the digitization, interpretation, and categorization of the magnetic lineaments into three classes was performed: a) local lineaments generated by the CET algorithm called *magnetic texture*; b) lineaments that cross MDs and show trends in length and shape, identified as *first-order lineaments*; and c) regional lineaments that separate MDs, called *magnetic lineaments*. Magnetic coverages, such as the tilt derivative, the total field magnetic anomaly (TMA), the reduction in the pole of the TMA and the MDs, were used as support.

Rose diagrams to evaluate the orientation of the lineaments were generated; these plots represent the direction of bearing and show the percentage of distribution of the data, according to the length of each lineament. This allows for the analysis and comparison of the characteristics of the magnetic lineaments identified in each area of interest (Figures 15 and 16).

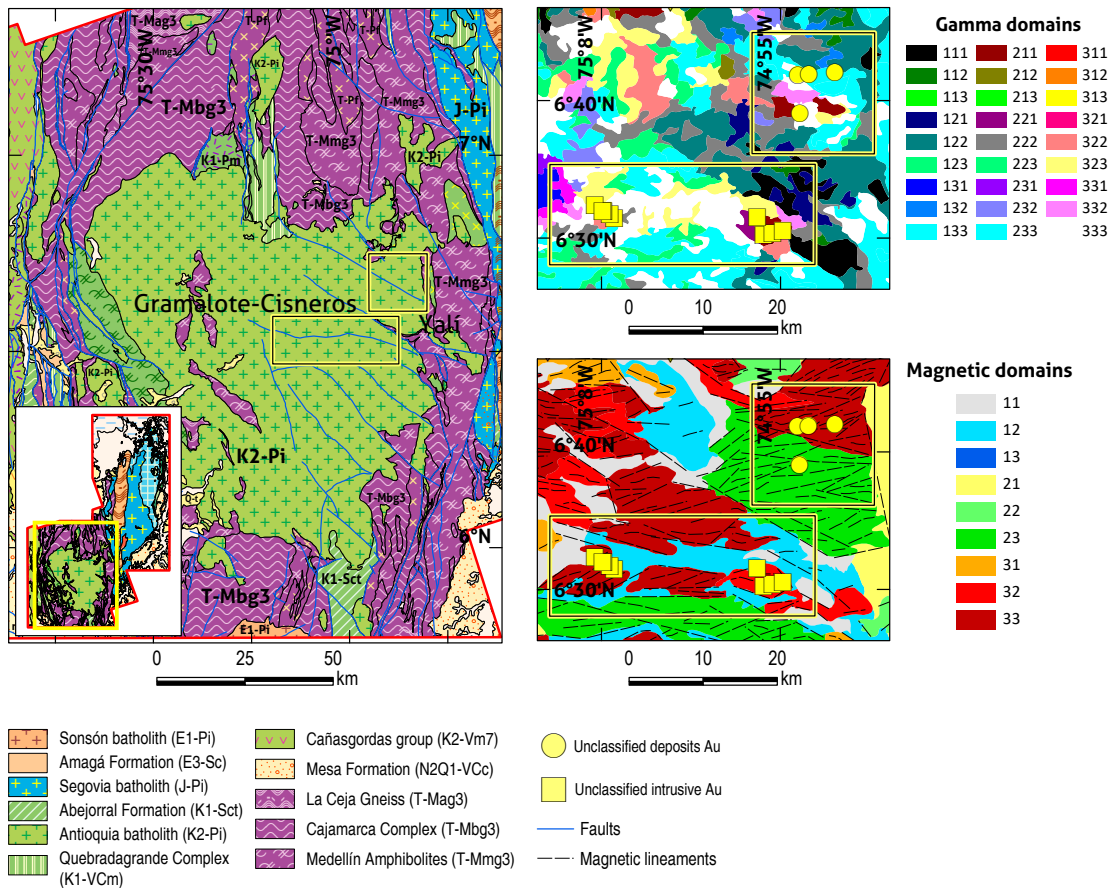


Figure 15. Geological-geophysical integration in the Gramalote and Yalí metallogenic districts. Left: geological units; right: gamma domains and magnetic domains.

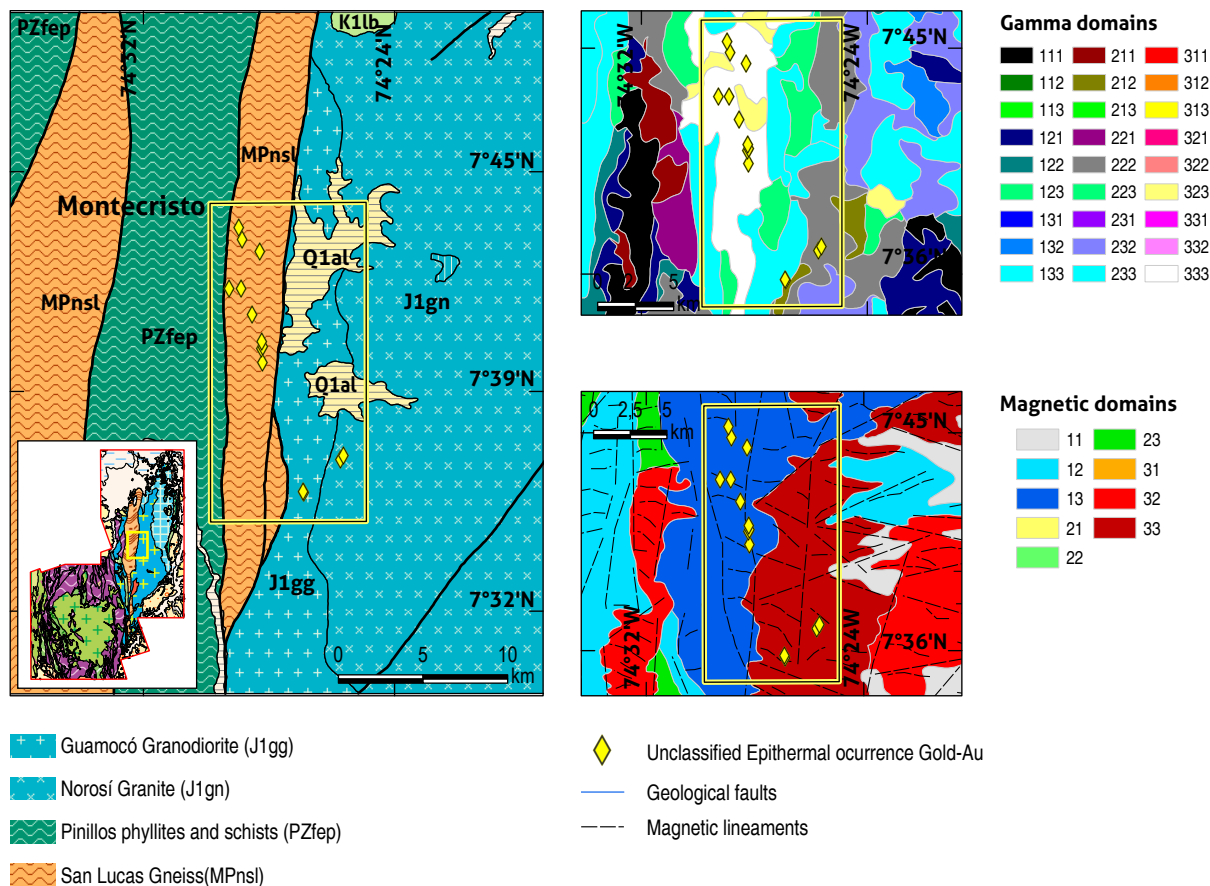


Figure 16. Geological-geophysical integration in the Monte Cristo metallogenic district. Left: San Lucas Gneiss (MPnsl), right: gamma domains and magnetic domains.

## 5. DISCUSSION AND EXAMPLES OF INTEGRATION WITH GEOLOGICAL INFORMATION

The integration of geophysical and geological data from the gamma spectrometric and magnetic domains with geological data for the Serranía San Lucas-Antioquia Batholith area and eastern Colombia (covered in large parts by sedimentary substrate) shows the contrast of a series of geophysical attributes associated with the different geological units. This information contributes to the geological knowledge, helps in the identification of areas with the potential to host mineral resources, and supports geological mapping. Some examples of this potential are presented below.

### 5.1. Hydrothermal alteration zones: Antioquia Batholith, Serranía de San Lucas and Middle Magdalena Valley

To the southwest of the study area is the Antioquia Batholith (K2-Pi) outcrops, composed predominantly of tonalite-grano-

diorites. The radiometric counts for K vary from medium to low and are high in U-Th. The GDs highlight some regions that present high K values (GD-322 and GD-311); these regions are probably associated with potassium alteration zones that coincide with unclassified gold deposits and intrusive rocks included in the Metallogenic Map of Colombia (Sepúlveda et al., 2020) in the metallogenic gold districts of Gramalote and Yalí (Figure 15). On the other hand, the MDs in this area show high intensities, with rough to intermediate textures (MD-33 and MD-32). These values could be associated with more recent intrusions within the Antioquia Batholith.

Figure 16 shows the Monte Cristo metallogenic district located in the Serranía de San Lucas. In this area, several gold deposits are present (unclassified epithermal type (Sepúlveda et al., 2020)); these deposits are located in the San Lucas Gneiss (MPnsl) that consist of hornblende and biotitic quartz-feldspathic gneisses. The area in which this unit is found includes the Pa-



lestina and Tigüí faults and coincides with high GD values (GD: 333, GD: 323). To the west of this unit, there are low GD values that coincide with phyllites and Pinillos schists. To the east of the Tigüí Fault, the Guamocó Granodiorite (J1gg) shows high values of U and Th. The MDs show a strong contrast between low magnetic intensities associated with the San Lucas Gneiss and high intensities associated with the Guamocó Granodiorite.

In the El Vapor metallogenic district, located in the Middle Magdalena Valley (Figure 17), gold occurrences (associated with unclassified intrusive rocks) were identified, oriented north-south between the El Bagre and Nus faults, which coincides with the GDs with high K values. This area has a good lithological contrast. For example, to the east, the Antioquia Batholith shows low gamma domains, and the graphite schists of muscovite quartz have high U values in contrast to the high K values of the Segovia Batholith, which are delimited by the Palestina Fault. To the east, the San Lucas Gneiss coincides with high U. On the other hand, the MDs indicate high inten-

sities with medium textures, and there is evidence of wedging in the magnetic lineaments west of the Palestina Fault, where the rocks with unclassified gold intrusions are located.

## 5.2. Magnetic lineaments and geological structures: Antioquia Batholith and Serranía de San Lucas

The magnetic lineaments in the Serranía de San Lucas area shows different trends. The most representative are the regional lineaments with azimuths between 0° and 30° located in the central part of the Serranía de San Lucas. These lineaments coincide with the Palestina Fault, whose general direction is north-south, and to the west, with the El Bagre Fault and the Nus Fault. Some of these lineaments seems to be included in the general orientation of the Palestina Fault and form a braided system of structures in this orientation.

To the east of the Palestina Fault, smaller magnetic lineaments are observed with azimuths that vary between 30° and 60°; these could correspond to satellite faults-detected features

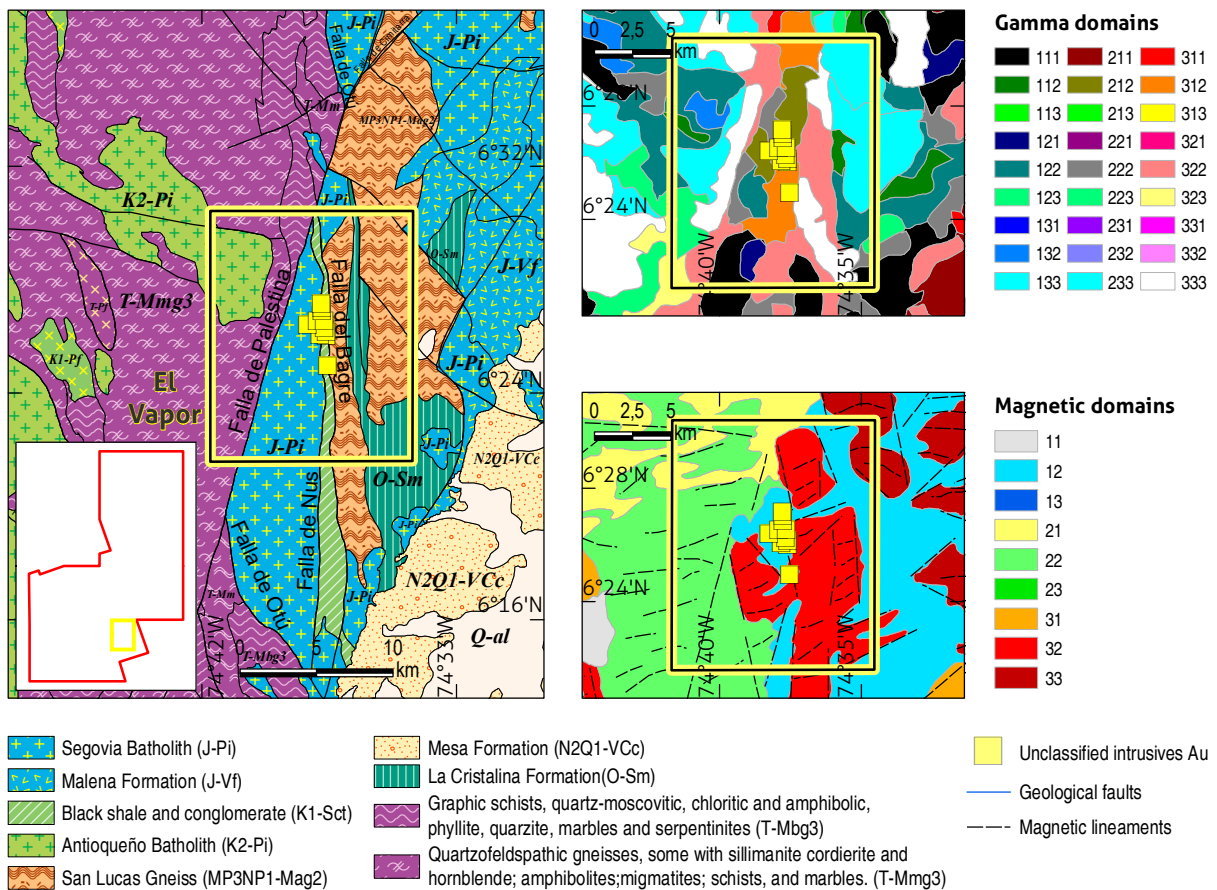


Figure 17. Geological-geophysical integration in the El Vapor metallogenic district. Left: chronostratigraphic units; right: gamma domains and magnetic domains.



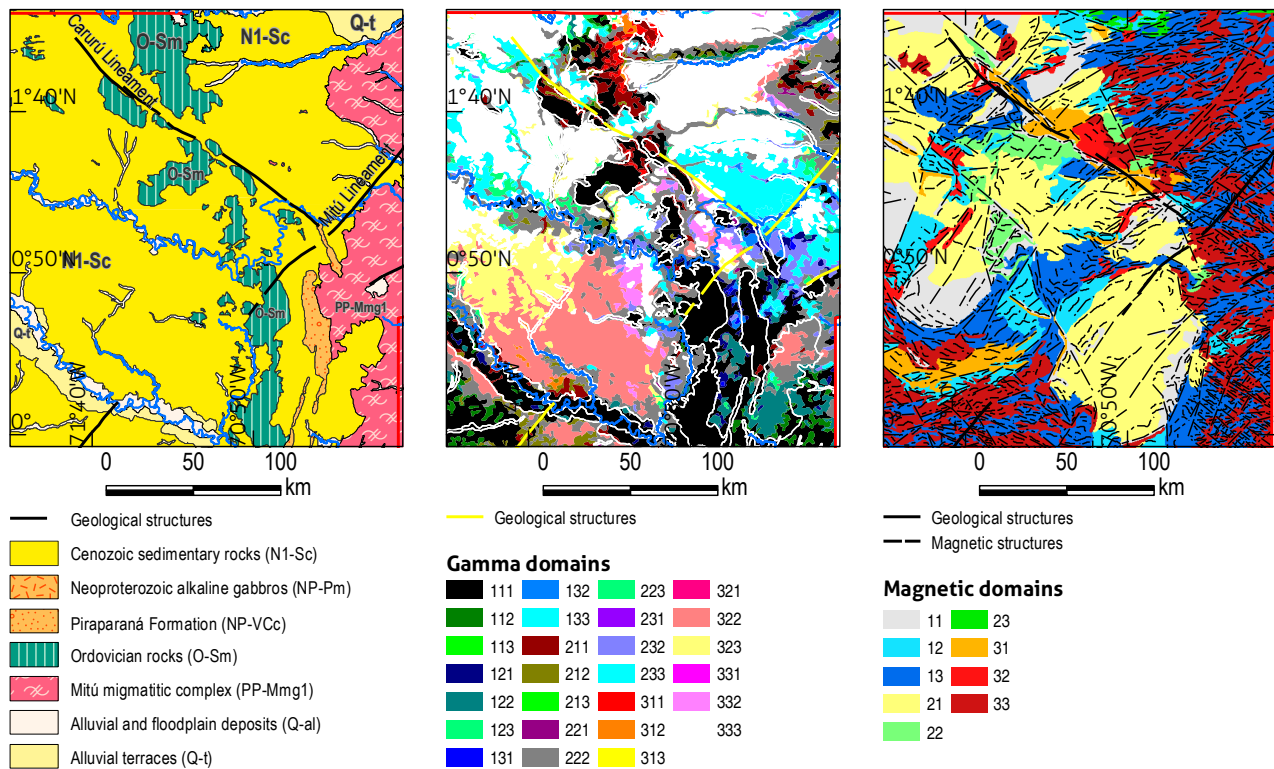


Figure 19. Geological-geophysical integration detailing the Ordovician units, gamma domains, and magnetic domains

ks within a unit. On the other hand, the gamma domains show the characteristics of the rock surfaces, which in many sectors indicate consistencies with the geological cartography and suggest that the rocks are good lithological markers.

## 6. CONCLUSIONS

Airborne geophysical data provides homogeneous coverage of the evaluated areas and enables the correlation of the geophysical responses of surface rocks and materials (Gamma spectrometry) and the subsoil (magnetometry) with the geological units and structures differentiated thus far in each unit.

The application of semiautomatic classification methodologies in the delimitation of magnetic domains and gamma spectrometric as well as for the automatic detection of lineaments is of great value in the integration and interpretation of large volumes of information that cover large areas. This is the case for the two areas evaluated here.

The integration of magnetic domains and gamma spectrometric domains with the regional geology of the area of the Serranía de San Lucas and Antioquia Batholith allowed to corre-

late the presence of regional faults, such as the Palestina Fault, and lateral contrasts in geochronological units known as the Antioquia Batholith and San Lucas gneiss. However, based on the interpretation of the geophysical domains, it is possible to point out changes and contrasts not reported in the geological cartography; these can be attributed to compositional changes in rocks, which in turn can indicate geological processes of alteration responsible for the accumulation of minerals of interest. An example of this was found in areas such as the El Vapor and Monte Cristo metallogenic districts.

Structural analysis was performed based on magnetometric information integrated with the geological cartography of the area of Serranía de San Lucas and the Antioquia Batholith. The correlation of lineaments and domains with main faults and variations in the orientation of secondary magnetic structures allowed the identification of different domains or blocks that must be explained from the point of view of geological evolution.

For eastern Colombia, information from gamma spectrometric domains represents a key tool in the review and adjustment of geological cartography. In addition, the lineaments and magnetic domains reflect high complexity and variation in

the predominantly magnetic rocks that make up the basement, both toward the easternmost part of the study area (where rocks are exposed) and toward the center of the study area (where basement rocks are covered by sedimentary rocks and recent deposits). Therefore, similar to the observations and correlations established in the San Lucas area, it is important to identify the interaction between structures of varying geological origin and possible compositional changes in response to the presence of rock units or alteration zones that have geological potential or metallogenic objects in more detailed studies.

The observations and interpretations presented in this work are based on the management of geophysical information and the preparation of thematic layers that can contribute to the geological mapping of the metallogenic potential of Colombia. Therefore, it is recommended to carry out complementary studies aimed at establishing the relationship between geophysical domains and geological units as well as identifying alteration zones, diagnostic features, or mineral accumulation processes.

## REFERENCES

- Abbass, A., & Mallam, A. (2013). Investigating the structures within the Lower Benue and Upper Anambra Basins, Nigeria, using first vertical derivative, analytical signal and (CET) Centre for Exploration Targeting plug-in. *Earth Sciences*, 2(5), 104-112. <https://doi.org/10.11648/J.EARTH.20130205.11>
- Gómez, J., Montes, N. E., Nivia, A., & Diederix, H. (comp.). (2015). *Mapa geológico de Colombia 2015. Escala 1:1 000 000*. Servicio Geológico Colombiano. <https://doi.org/10.32685/10.143.2015.935>
- Gunn, P. J., Maidment, D., & Milligan, P. R. (1997). Interpreting aeromagnetic data in areas of limited outcrop. *AGSO Journal of Australian Geology and Geophysics*, 17(2), 175-185.
- International Atomic Energy Agency. (2003). *Guidelines for radioelement mapping using gamma ray spectrometry data*. IAEA-TECDOC-1363.
- Isles, D. J., & Rankin, L. R. (2013). *Geological interpretation of aeromagnetic data*. Society of Exploration Geophysicists and the Australian Society of Exploration Geophysicists. <https://doi.org/10.1190/1.9781560803218>
- Japan Association on Remote Sensing. (1993). *Remote sensing note*.
- Killeen, P. G., Mwenifumbo, C. J., & Ford, K. L. (2015). Tools and techniques: Radiometric methods. *Treatise on Geophysics*, 11, 447-524. <https://doi.org/10.1016/B978-0-444-53802-4.00209-8>
- Marangoni, Y. R. (2014). AGG0324 - Métodos Potenciais. Parte 3: O Campo Magnético Conceitos e aplicações em Geofísica. In G. e. Universidade de São Paulo. Instituto de Astronomia, AGG0324 - *Métodos Potenciais* (pp. 24-33). São Paulo: Universidade de São Paulo.
- Martelet, G., Truffert, C., Tourlière, B., Ledru, P., & Perrin, J. (2006). Classifying airborne radiometry data with Agglomerative Hierarchical Clustering: A tool for geological mapping in context of rainforest (French Guiana). *International Journal of Applied Earth Observation and Geoinformation*, 8(3), 208-223. <https://doi.org/10.1016/J.JAG.2005.09.003>
- Miller, H. G., & Singh, V. (1994). Potential field tilt—a new concept for location of potential field sources. *Journal of Applied Geophysics*, 32(2-3), 213-217. [https://doi.org/10.1016/0926-9851\(94\)90022-1](https://doi.org/10.1016/0926-9851(94)90022-1)
- Moyano, I., Lara, N., Arias, H., Gómez, E., Ospina, D., Puentes, M., Robayo, A., Rojas, O., & Torrado, S. (2020). *Mapa de anomalías geofísicas de Colombia para recursos minerales, versión 2020*. Servicio Geológico Colombiano.
- Reeves, C. (2005). *Aeromagnetic surveys: Principles, practice, and interpretation*. Geosoft.
- Richards, J. A. (2013). Supervised classification techniques. In *Remote sensing digital image analysis*. Springer. [https://doi.org/10.1007/978-3-642-30062-2\\_8](https://doi.org/10.1007/978-3-642-30062-2_8)
- Sepúlveda, J., Celada, C. M., Leal-Mejía, H., Murillo, H., Rodríguez, A., Gómez, M., Prieto, D., Jiménez, C. A., Rache, A., & Hart, C. (2020). *Mapa metalogénico de Colombia 2020*. Memoria explicativa. Servicio Geológico Colombiano.
- Thébault, E., Finlay, C. C., Beggan, C. D., Alken, P., Aubert, J., Barrois, O., Bertrand, F., Bondar, T., Boness, A., Brocco, L., Canet, E., Chambodut, A., Chulliat, A., Coisson, P., Civet, F., Du, A., Fournier, A., Fratter, I., Gillet, N., ... Zvereva, T. (2015). International Geomagnetic Reference Field: the 12th generation. *Earth, Planets and Space*, 67, 79. <https://doi.org/10.1186/s40623-015-0228-9>
- Yang, C., Yang, C., Kao, S., Lee, F., & Hung, P. (2004). Twelve different interpolation methods: A case study of Surfer 8.0. In *Proceedings of the XXth ISPRS Congress* (pp. 778-785). <http://citeseerx.ist.psu.edu/viewdoc/summary?doi=10.1.1.183.7288>